Desalination and Water Treatment
www.deswater.com

47 (2012) 228–234
September

Taylor & Francis
Taylor & Francis Group

doi: 10.1080/19443994.2012.696404

Photocatalytic degradation of an azo dye Direct Sky Blue 5B in water: a comparative study using nanostructured ITO, ZnO, and ZnO/ITO thin films

Mojtaba Nasr-Esfahani

Department of Materials Science and Engineering, Najafabad Branch, Islamic Azad University, Najafabad 85141-43131, Iran
Tel. +98 311 2356771; Fax: +98 311 2356771; email: m-nasresfahani@iaun.ac.ir

Received 12 February 2011; Accepted 27 March 2012

ABSTRACT

Indium tin oxide (ITO), zinc oxide (ZnO), and ZnO/ITO interface composite thin films were deposited on glass substrates using electron-beam evaporation and the sol–gel method. The porous 2%PEG–ZnO/ITO thin films were also have been prepared using the polyethylene glycol (PEG) as an organic template. The samples were characterized by UV–Vis spectroscopy, X-ray diffraction, and scanning electron microscopy techniques. The photocatalytic degradation of Direct Sky Blue 5B in an aqueous solution, as a model compound, was investigated using different catalysts in an attempt to compare the decomposition reaction rates. The effects of various experimental parameters, such as an initial concentration of the Direct Sky Blue 5B (5–10 mg/l), pH of the solution (4–9), and catalytic nature and its microstructure, were systematically studied to achieve the maximum degradation efficiency. The results obtained were fitted with the Langmuir–Hinshelwood model to study the degradation kinetics and were discussed in detail. Degradation with 2%PEG–ZnO/ITO was more efficient than with ITO, ZnO, and ZnO/ITO films.

Keywords: Photocatalytic degradation; Sol–gel; Direct Sky Blue 5B; Nanostructure; ZnO; ITO

1. Introduction

Textile wastewater contains several residual dyes that are not readily biodegradable [1]. Methods applied to purify the textile waste water such as common chemical oxidation are fraught with serious drawbacks, including the high cost of by-products or their hazardous nature. In the past two decades, the photocatalytic activity of the oxide semiconductors (e.g. TiO_2 [2–5], ZnO [6–8], ITO [9]) was developed to degrade organic compounds in the industrial wastewater (e.g. dyes, alkanes, alkenes, pesticides, herbicides, aromatics [10,11]). Compared to other conventional means to treat wastewater, this technology employing photocatalytic activity boasts of a number of advantages mentioned below: (1) it has a wide gamut of applications, especially to molecule–structure complex contaminants, which cannot be easily degraded by the traditional methods, (2) the oxide semiconductor itself does not show any toxicity to human beings, and (3) it demonstrates a strong destructive power on the pollutants and can even mineralize the pollutants into CO_2 and H_2O.

Among the oxide semiconductors that are used for photodegradation, ZnO has a few privileges over others such as: generating H_2O_2 more efficiently, having high reaction and mineralization rates and having a many active sites with high surface reactivity [12]. On the other hand, ZnO has been used as a photocatalyst for the degradation of various pollutants due to its higher quantum efficiency than TiO_2 [13,14]. The use of nanostructured ZnO films also has two advantages in comparison with the particles; (1) saving energy and time, and (2) having a high surface-to-volume ratio, which enhance the photocatalytic activity [15].

As another well-known photocatalyst, the tin-doped indium oxide (known as indium tin oxide or ITO) material has also received much attention for the degradation of various environmental pollutants [16]. This reason behind the preference for ITO lies in the use ful optical and electrical properties of the ITO, which make it very well suited for the transparent conducting electrodes that are used in photoelectrocatalytic degradation. In addition, the band gap energy of ITO is similar to that of ZnO (i.e. ~3.2–3.5 eV) [17,18]. Thus, it is possible to enhance the photocatalytic activity of the ZnO photocatalyst by applying the ITO interface coating.

In continuation of our ongoing programme to develop thin solid films for photocatalytic purposes [19–23], in the present study we report a detailed investigation on the ZnO/ITO interface nanofilms. Porous ZnO and ZnO/ITO nanofilms were then produced via the sol–gel process using polyethylene glycol (PEG) as the organic template and glass slide as the substrate. Then, semiconductor photocatalysts (ITO, ZnO, ZnO/ITO, and 2%PEG–ZnO/ITO nanofilms) were compared according to the decolorization efficiency of an aqueous solution of Direct Sky Blue 5B.

2. Experimental

2.1. Materials

The following reagents were used to prepare the sol: zinc acetate dihydrate ($Zn(OOCCH_3)_2{\cdot}2H_2O$, 98%, Aldrich), monoethanolamine (MEA, Merck), 2-methoxyethanol (Merck), and polyethylene glycol ($M_{av} = 1500$, PEG, Aldrich). The water used in the experiments was of the double-distilled deionized type.

2.2. Film preparation

The precursor sol was prepared by dissolving the zinc acetate dihydrate ($Zn(CH_3COO)_2{\cdot}2H_2O$) in 2-methoxyethanol followed by adding monoethanolamine (MEA) into the solution. We used 2-methoxyethanol as the solvent, but MEA concentration had a great influence on the solution's stability. So, several precursor sols were prepared by altering the ratio of $Zn(Ac)_2{\cdot}2H_2O$:MEA. The most stable sol was then obtained with the $Zn(Ac)_2{\cdot}2H_2O$:MEA molar ratio of 1:1 in 2-methoxyethanol. In fact, we found that the sol prepared with this composition was stable for at least 30 days. It should be pointed out the concentration of the total metal ions was 0.35 M, and the molar ratio of MEA to the total metal ions in the solution was kept constant at 1.0 in the above mentioned precursor sol. The solution became clear after being stirred for a while at room temperature. PEG was then added and the solution was additionally stirred for 2 h until a transparent sol was obtained again. The best amount of PEG addition was 2 wt.% of the ZnO sol, as discussed elsewhere [24].

To prepare the substrate, a low-level tin-doped indium oxide (ca. 10 wt.% SnO_2) film was deposited on the glass substrate (softening point, 600°C) by the electron-beam technique (Iranian Optical Co.). The thickness of the ITO film was 120 nm, as measured using a quartz crystal thickness monitor. The film was heat-treated at 550°C in air to enhance its crystallinity. The ZnO film was then spin-coated at 1,200 rpm onto the prepared substrate, and dried for 10 min on a hot plate at 100°C to evaporate the solvent and remove organic residuals. The whole procedure, from coating to drying, was repeated four times to thicken the ZnO films. The final layer was annealed for 60 min in air, at 550°C.

2.3. Catalyst characterization

2.3.1. Optical properties

Transmittance of the prepared films was determined using a Varian Cary 500 spectrophotometer in the wavelength range of 300–800 nm. The optical transmittance higher than 75% in the visible region of spectrum was obtained for all films. A comparison of the transmittance spectra of ITO, ZnO, and ZnO/ITO films (Fig. 1) showed that the ZnO/ITO film exhibits a stronger absorption in the visible light region than the ITO and ZnO films. Furthermore, a red shift of absorption threshold was observed for the ZnO/ITO film in comparison with the ITO and ZnO films. An increase in absorption threshold for a semiconductor signifies a decrease in its band gap energy, resulting in high use of solar spectrum. Therefore, it is anticipated that the ZnO/ITO film should show a higher photocatalytic activity than the pure ITO and ZnO films. Further studies are being carried out to investigate this effect.

2.3.2. Morphological properties

The surface morphology of the films was analyzed using a scanning electron microscope (SEM; Philips XL30, voltage 20 kV). The scanning electron micro-

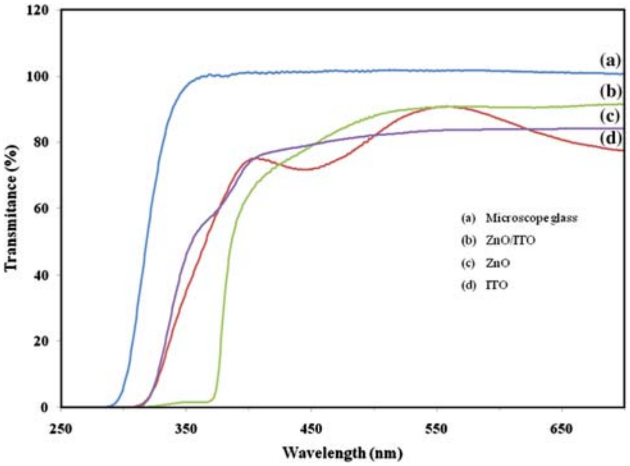

Fig. 1. Transmission spectra of (a) glass slide, (b) ITO, (c) ZnO, (d) ZnO/ITO films.

scope (SEM) images of the three samples after calcinations at 550℃ are shown in Fig. 2. Some cracks were visible for the ZnO/ITO film deposited without PEG. A more rough surface marked by grains with a higher average size was observed for the ZnO/ITO film without PEG. Small grains with a dense structure and proper surface coverage were observed for other films. The ZnO/ITO film was obtained with 2 wt.% PEG addition, and it is clear from the image that the ZnO particle size lies between 30 and 40 nm. One of these nanoparticles is marked in Fig. 2 by a multiplication sign, ×.

2.3.3. Structural studies

The X-ray diffraction (XRD) patterns were obtained on a D8 Advanced Bruker X-ray diffractometer using Cu Kα radiation at an angle of 2θ from 10 to 100. Fig. 3 shows the XRD patterns of films annealed at 550℃. All as-deposited films were almost amorphous or nanocrystalline. However, all of the samples crystallized when the annealing temperature ranged between 450 and 550 ℃. Fig. 3(a) shows the XRD pattern of an ITO thin film after the physical vapor deposition on the glass substrate and heat treatment at 550° C. The ITO film exhibits cubic lattice crystal structure, preferential orientation in (222). Fig. 3(b) and (c) also shows the XRD patterns of ZnO/ITO thin films with and without PEG after heat treatment at 550℃, respectively. Both the figures exhibit the fact that a crystalline ITO film has formed on the glass substrate, and ZnO/ITO films were successfully prepared, showing that PEG is substantially free of the substance that could induce the crystallization of ZnO during any of the densification steps.

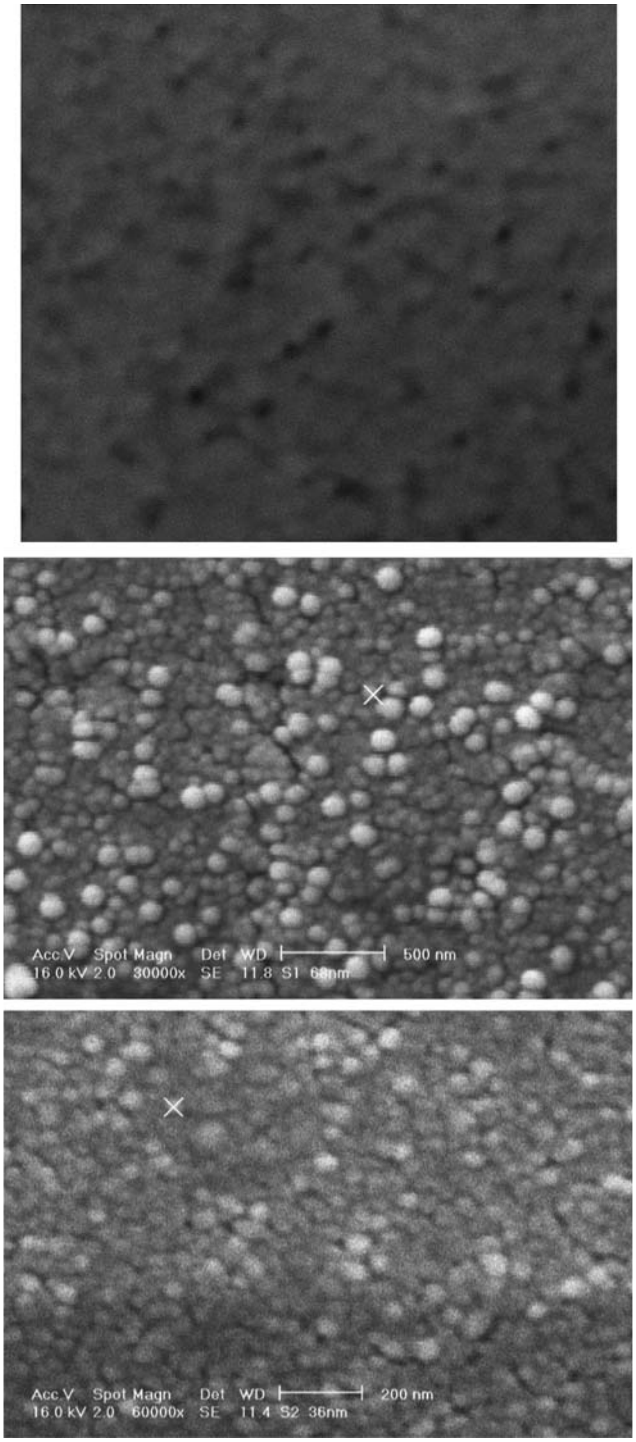

Fig. 2. SEM images of (a) ITO, (b) ZnO/ITO and (c) PEG–ZnO/ITO films.

The particle sizes of the prepared films were calculated using the Scherrer Eq. $D = k\lambda/B\cos\theta$; where $k = 0.9$ is a coefficient, $\lambda = 1.541$ Å is the X-ray wavelength, B is the full-width at half-maximum of the film and θ is the diffracting angle. The calculated nanopar-

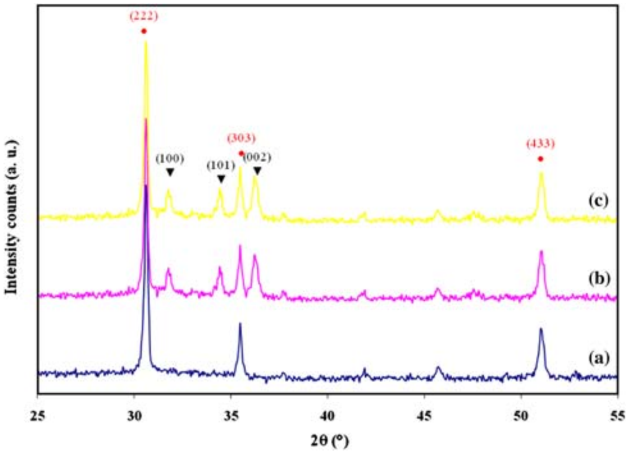

Fig. 3. (a) X-ray diffraction patterns of (a) ITO, (b) ZnO/ITO and (c) PEG–ZnO/ITO films. Black triangles denote the characteristic peaks of ZnO and the circles denote the peaks of ITO.

ticle sizes of films annealed at 550℃ were accordingly: ITO (60 nm), ZnO/ITO without PEG (45 nm), and ZnO/ITO with 2 wt.% PEG (24 nm).

2.4. *Photocatalytic activity measurements*

To evaluate the catalytic activity of ITO, ZnO, ZnO/ITO, and 2%PEG–ZnO/ITO thin films, the photodegradation of a well-known organic azo dye Direct Sky Blue 5B (Fig. 4) was investigated as a simple model compound under UV irradiation. The dye solution with the desired concentration was prepared in double-distilled water. For the irradiation experiment, 20 mL of aqueous solution was taken in the photoreactor. The pH of the reaction mixture was adjusted by adding a dilute aqueous solution of either HCl or NaOH. We irradiated both ITO, ZnO, ZnO/ITO, and 2%PEG–ZnO/ITO films with a 200 W high-pressure mercury lamp at 15 cm from the top of the model solution. The solution was continuously stirred in a constant-temperature water bath at 25℃. Then we drew 4-milliliter samples at regular time intervals during irradiation. The samples were analyzed by a double-beam UV–vis spectrophotometer (UV-2550 UV–visible Spectrophotometer SHIMADZU) to measure the concentration of the dye at 612 nm.

The decrease in the absorbance value of samples at $\lambda_{\max}$ of the dye after irradiation in a certain time interval indicates the rate of decolorization and, therefore, indicates the photodegradation efficiency of the dyes as well as the photocatalytic activity. The decolorization and degradation efficiency have been calculated as:

$$\text{Efficiency} = 100\left(\frac{C_0 - C}{C_0}\right)$$

where C_0 is the initial concentration of the dye and C is the concentration of the dye after irradiation in the selected time interval.

3. Results and discussion

3.1. *Effect of UV irradiation and metal oxide semiconductor*

In an aqueous solution, the photoassisted catalytic degradation of the dyes is triggered by the active species that is produced on the surface of the metal oxide semiconductors. Under UV irradiation of proper energy, the photogenerated electron–hole pair has a lifetime in the space charge region that enables its involvement in chemical reactions. The heterogeneous photocatalysis takes place after a partial or a complete mineralization of the many organic pollutants following the proposed mechanism:

$$\mathrm{SC} + hv \rightarrow \mathrm{SC}(h^+_{\mathrm{VB}} + e^-_{\mathrm{CB}}) \tag{1}$$

$$\mathrm{OH}^-_{\mathrm{ads}} + h^+_{\mathrm{VB}} \rightarrow {}^{\cdot}\mathrm{OH}_{\mathrm{ads}} \quad \text{(in basic medium)} \tag{2}$$

$$\mathrm{H_2O_{ads}} + h^+_{\mathrm{VB}} \rightarrow {}^{\cdot}\mathrm{OH}_{\mathrm{ads}} + \mathrm{H}^+ \tag{3}$$

Electron in the conduction band (e^-_{CB}) on the catalyst surface can reduce the molecular oxygen to a superoxide anion:

$$\mathrm{O}_{2(\mathrm{ads})} + e^-_{\mathrm{CB}} \rightarrow {}^{\cdot}\mathrm{O}^-_{2(\mathrm{ads})} \tag{4}$$

This radical is also responsible for the production of hydroxyl and hydrogen peroxides radicals:

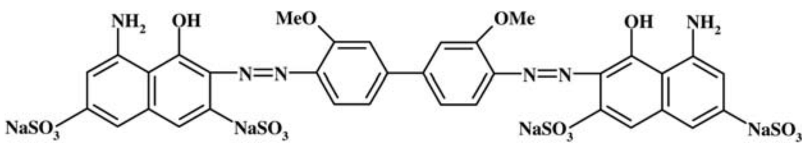

Fig. 4. Chemical structure of commercial diazo dye of Direct Sky Blue 5B (C. I. Direct Blue 15).

$$^{\bullet}O^{-}_{2(ads)} + H^{+} \rightarrow HO^{\bullet}_{2(ads)} \quad \text{(in acidic medium)} \tag{5}$$

$$2HO^{\bullet}_{2(ads)} \rightarrow O_2 + H_2O_2 \tag{6}$$

$$H_2O_2 + {}^{\bullet}O^{-}_{2(ads)} \rightarrow O_2 + HO^{\bullet} + HO^{-} \tag{7}$$

$$^{\bullet}O^{-}_{2(ads)} + HO^{\bullet}_{2(ads)} + H^{+} \rightarrow H_2O_2 + O_2 \tag{8}$$

Hydroxyl ($HO^{\bullet}$), hydrogen peroxides ($HO^{\bullet}_2$), and superoxide ($^{\bullet}O_2^{-}$) radicals are highly reactive species that will oxidize the organic compounds adsorbed on the semiconductor surface. However, the high oxidative potential of the hole (h^{+}_{VB}) in the catalyst permits the direct oxidation of organic matter (dye) to reactive intermediates:

$$\text{dye} + h^{+}_{VB} \rightarrow \text{dye}^{\bullet +} \rightarrow \text{oxidation of dye} \tag{9}$$

3.2. Comparison of the photocatalytic activity

First, control tests showed that the adsorption of the dye in the reactor vessel was negligible and that a small amount of the Direct Sky Blue 5B was degraded by photolysis (absence of photocatalytict films Fig. 5 (×)) from the lower wavelength UV radiation. Next, the photocatalytic experiments were carried out using different catalysts at fixed pH value and dye concentration (pH = 4.7, 5 mg/l). Then, the degradation efficiencies of different semiconductors were compared to select the most effective catalyst for the degradation of the dye. Fig. 5 shows the variation of decolorization percentage of Direct Sky Blue 5B using different catalysts under the UV irradiation, after deducting both physical adsorption and the self-degradation of Direct Sky Blue 5B under UV.

The results indicated that 2%PEG–ZnO/ITO exhibits a higher photocatalytic activity than others. In this regard, the observed photocatalytic efficiency increased in the following order: ITO<ZnO<ZnO/ITO<2%PEG–ZnO/ITO.

The difference between the photoactivities of the four samples is possibly due to their different microstructures, as shown from the SEM results. It seems a great ability to capture photons is exhibited efficiently by the nanocrystalline 2%PEG–ZnO/ITO film due to its rough and high surface area. On the other hand, an increase in the absorption threshold for a semiconductor means a decrease in its band gap energy, resulting in the high use of the solar spectrum. Therefore, it is anticipated that a ZnO/ITO film should show a higher photocatalytic activity than the pure ZnO and ITO films.

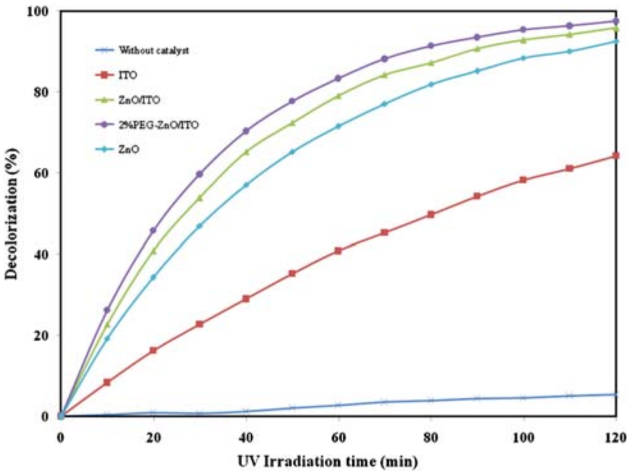

Fig. 5. Decomposition of Direct Sky Blue 5B dye solution at 4.7 pH without photocatalyst (×) and in the presence of ITO (■), ZnO (◆), ZnO/ITO (▲) and 2%PEG–ZnO/ITO (●) thin films.

However, the higher rate of degradation over ZnO/ITO and 2%PEG–ZnO/ITO supports the view that the optical property (band gap) is as important as the surface-mediated process in the degradation reaction.

3.3. Effect of pH solution

To find the optimal pH of the reaction mixture for the photodegradation of Direct Sky Blue 5B, a series of experiments were carried out using different pHs. The results are presented in Fig. 6. As it can be observed, the pH value of a Direct Sky Blue 5B solution had significant influence on the photocatalytic activity of the ZnO/ITO film. It is also an important operational variable in the actual wastewater treatment. The decrease in the pH of Direct Sky Blue 5B solution led to enhanced efficiency in the degradation of Direct Sky Blue 5B. The interpretation of pH effect on the photocatalytic process is very difficult owing to its multiple roles such as electrostatic interactions between the semiconductor surface, solvent molecules and substrate, and charged radicals formed during the reaction process. The amphoteric behavior of the semiconductor causes the surface charge property of metal oxide thin films to change with the solution pH. For nanosized ZnO, the pH_{zpc} (zero point charge) is known to be 9 [25]. Since the semiconductor is positively charged at low pH levels, it adsorbs the negatively charged Direct Sky Blue 5B owing to the

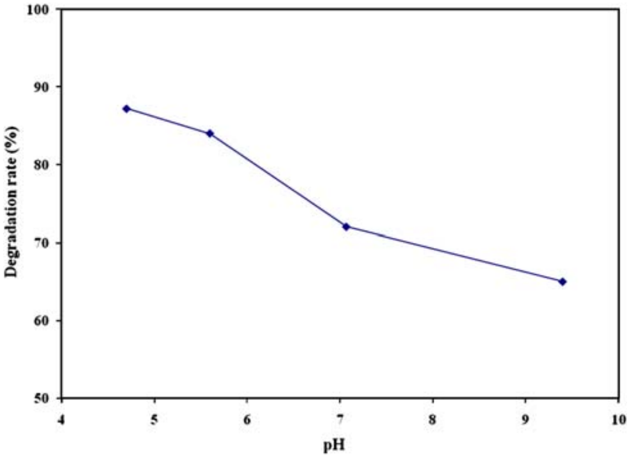

Fig. 6. Effects of pH value on photocatalytic degradation of Direct Sky Blue 5B after 80 min.

Coulombic attraction, which favors the interaction of hole or hydroxyl radicals with Direct Sky Blue 5B molecules.

3.4. Kinetic analysis

In this section, a series of Direct Sky Blue 5B solutions was prepared with initial dye concentrations of about 5, 8 and 10 mg/L at pH 4.7, and the photocatalytic efficiency was measured for the 2%PEG–ZnO/ITO film. Generally, the photodegradation rates of chemical compounds on semiconductor surfaces follow the Langmuir–Hinshelwood model [26–29] because the absorption of the organic species on the thin film surface is the controlling step in the whole degradation process. The relationship between the initial concentration of Direct Sky Blue 5B and the illumination time is plotted in Fig. 7 for the degradation reaction catalyzed by the 2%PEG–ZnO/ITO film. The results show that the kinetics of photocatalytic reaction fits the Langmiur–Hinshelwood kinetics model well. Therefore, the absorption of Direct Sky Blue 5B on the thin film surface is the controlling step in the whole degradation process.

The degradation rate is directly proportional to the probability of the formation of hydroxyl radicals ($^{\bullet}$OH) on the catalyst surface and the probability of hydroxyl radicals reacting with the dye molecules. The interaction of $^{\bullet}$OH radical with dye decreases as the initial concentration of the dye increases. Furthermore, the increase in the dye concentration also reduces the relative formation of both hydroxyl radicals and superoxide radical anions due to reduced light penetration to the solution, leading to decrease in the photodegradation efficiency.

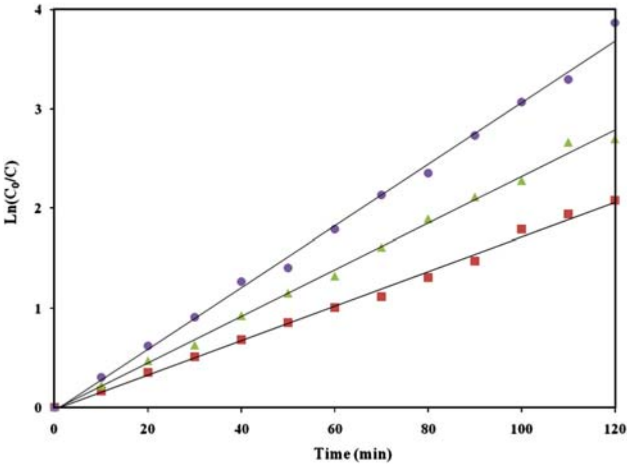

Fig. 7. Photodegradation kinenetic of Direct Sky Blue 5B using 2%PEG–ZnO/ITO at different dye concentrations and pH 4.7: (●) $[C_o] = 5$ (mg/l) (rate constants = 0.030 min^{-1}, (▲) $[C_o] = 8$ (mg/l) (rate constant = 0.023 min^{-1}) and (■) $[C_o] = 10$ (mg/l) (rate constant = 0.017 min^{-1}).

4. Conclusion

In the present study, nanostructured ZnO, ZnO/ITO, and 2%PEG–ZnO/ITO films were prepared using the sol–gel process. The Direct Sky Blue 5B decomposition kinetics was studied experimentally by varying the photocatalysts, initial dye concentration, and solution pH. The results of the present study revealed that the 2%PEG–ZnO/ITO interface composite film was a more efficient photocatalyst for the photocatalytic decomposition of Direct Sky Blue 5B than ITO, ZnO, and ZnO/ITO at the given conditions. This phenomenon may be due to factors such as: (1) the higher surface area of 2%PEG–ZnO/ITO film compared to that of others; (2) an increase in the absorption threshold for ZnO/ITO, which means a decrease in its band gap energy, resulting in the high use of solar spectrum. The extent of degradation of Direct Sky Blue 5B was also influenced by the pH. Acidic pH found to be the best parameter for carrying out photocatalytic degradation. The decomposition rate decreased with an increase in the initial dye concentration. Finally, kinetic studies revealed that photodecolorization followed pseudo-first order kinetics with respect to dye concentration.

Acknowledgments

The author wish to thank the Najafabad Branch, Islamic Azad University for financially supporting this work.

References

[1] M.H. Habibi, Photocatalytic mineralisation of four model azo dyes in the presence of nanocomposite thin film Pt/ZnO catalysts coated on glass from aquatic environment, Int. J. Environ. Stud. 67 (2010) 393–403.

[2] K. Okamoto, Y. Yamamoto, H. Tanaka, M. Tanaka, A. Itaya, Heterogeneous photocatalytic decomposition of phenol over TiO_2 powder, Bul. Chem. Soc. Jpn. 58 (1985) 2015.

[3] V. Augugliaro, L. Palmisano, A. Sclafani, C. Minero, E. Pelizzetti, Photocatalytic degradation of phenol in aqueous titanium dioxide dispersions, Toxicol. Environ. Chem. 16 (1988) 89–109.

[4] H. Al-Ekabi, N. Serpone, Kinetics studies in heterogeneous photocatalysis. I. Photocatalytic degradation of chlorinated phenols in aerated aqueous solutions over titania supported on a glass matrix, J. Phys. Chem. 92 (1988) 5726–5735.

[5] M. Barbeni, E. Pramauro, E. Pelzzetti, E. Borgarell, M. Gratzel, N. Serpon, Photodegradation of pentachloro phenol catalyzed by titanium dioxide particles, Chemisorpe 14 (1985) 195–207.

[6] C.A.K. Gouveêa, F. Wypych, S.G. Moraes, N. Durán, N. Nagata, P. Peralta-Zamora, Semiconductor-assisted photocatalytic degradation of reactive dyes in aqueous solution, Chemosphere 40 (2000) 433.

[7] C. Lizama, J. Ferrer, J. Baeza, H.D. Mansilla, Optimized photodegradation of Reactive Blue 19 on TiO_2 and ZnO suspensions, Catal. Today 76 (2002) 235.

[8] M.A. Behnajady, N. Modirshahla, N. Daneshvar, M. Rabbani, Photocatalytic degradation of C.I. Acid Red 27 by immobilized ZnO on glass plates in continuous-mode, J. Hazard. Mater. 140 (2007) 257–263.

[9] H. Yumoto, T. Inoue, S.J. Li, T. Sako, K. Nishiyama, Application of ITO films to photocatalysis, Thin Solid Films 345 (1999) 38–41.

[10] A.G.S. Prado, L.L. Costa, Photocatalytic decouloration of malachite green dye by application of TiO_2 nanotubes, J. Hazard. Mater. 169 (2009) 297–301.

[11] M.V.P. Sharma, G. Sadanandam, A. Ratnamala, V.D. Kumari, M. Subrahmanyam, An efficient and novel porous nanosilica supported TiO_2 photocatalyst for pesticide degradation using solar light, J. Hazard. Mater. 171 (2009) 626–633.

[12] B. Pare, P. Singh, S.B. Jonnalagadda, Visible light induced heterogeneous advanced oxidation process to degrade pararosanilin dye in aqueous suspension of ZnO, Indian. J. Chem. A 47 (2008) 830–835.

[13] M.J. Height, S.E. Pratsinis, O. Mekasuwandumrong, P. Praserthdam, Ag-ZnO catalysts for UV-photodegradation of methylene blue, Appl. Catal. B: Environ. 63 (2006) 305–312.

[14] A.A. Khodja, T. Sehili, J.-F. Pilichowski, P. Boule, Photocatalytic degradation of 2-phenylphenol on TiO_2 and ZnO in aqueous suspensions, J. Photochem. Photobiol. A 141 (2001) 231–239.

[15] E. Rego, J. Marto, P.S. Marcos, J.A. Labrincha, Decolouration of Orange II solutions by TiO_2 and ZnO active layers screen-printed on ceramic tiles under sunlight irradiation, Appl. Catal. A 355 (2009) 109–114.

[16] M.H. Habibi, N. Talebian, Photocatalytic degradation of an azo dye X6G in water: A comparative study using nanostructured indium tin oxide and titanium oxide thin films, Dyes Pigments 73 (2007) 186–194.

[17] D.K. Zhang, Y.C. Liu, Y.L. Liu, H. Yang, The electrical properties and the interfaces of Cu_2O/ZnO/ITO p–i–n heterojunction, Physica B 351 (2004) 178–183.

[18] W. Shouqiang, S. Zhongcai, L. Xudong, L. Ying, C. Linlin, H. Yan, Photocatalytic degradation of methyl orange over ITO/CdS/ZnO interface composite films, J. Environ. Sci. 21 (2009) 991–996.

[19] M.H. Habibi, M. Nasr-Esfahani, Preparation, characterization and photocatalytic activity of a novel nanostructure composite film derived from nanopowder TiO_2 and sol–gel process using organic dispersant, Dyes Pigments 75 (2007) 714–722.

[20] M. Nasr-Esfahani, M.H. Habibi, A comparative study on physicochemical properties and photocatalytic behavior of two different nanostructure composite TiO_2 films coated on glass substrate, Desalin. Water Treat. 3 (2009) 64–72.

[21] M. Nasr-Esfahani, M.H. Habibi, Comparison of physicochemical properties of three nanostructure composite TiO_2 films and their photocatalytic properties, J. Nanosci. Nanotechnol. 10 (2010) 1159–1165.

[22] M. Nasr-Esfahani, M.H. Habibi, Photochemical characterization and photocatalytic properties of a nanostructure composite TiO2 film, Inter. J. Photoenergy (2008), Article ID 628713, 11.

[23] M. Nasr-Esfahani, A. Khakifirooz, N. Tavakoli, M.H. Soleimani, Preparation, characterization and photocatalytic activity of a novel nanostructure ZnO composite film derived sol–gel process using organic binder materials, Desalin. Water Treat. 21 (2010) 202–209.

[24] M. Nasr-Esfahani, A. Nourmohammadi, ZnO/ITO interface nanostructure films for the photocatalytic degradation of a textile dye, Reac. Kinet. Mech. Cat. (2012) in press.

[25] A. Akyol, H.C. Yatmaz, M. Bayramoglu, Photocatalytic decolorization of Remazol Red RR in aqueous ZnO suspensions, Appl. Catal. B: Environ. 54 (2004) 19–24.

[26] X.H. Qi, Z.H. Wang, Y.Y. Zhang, Y. Yu, J.L. Li, Study on the photocatalysis performance and degradation kinetics of X-3B over modified titanium dioxide, J. Hazard. Mater. 118 (2005) 219–225.

[27] D. Dvoranoval, V. Brezova, M. Mazur, M.A. Malati, Investigations of metal-doped titanium dioxide photocatalysts, Appl. Catal. B 37 (2002) 91–105.

[28] F. Kiriakidou, D.I. Kondarides, X.E. Verykios, The effect of operational parameters and TiO2-doping on the photocatalytic degradation of azo-dyes, Catal. Today 54 (1999) 119–130.

[29] A. Sobczýnski, L. Duczmal, W. Zmudínski, Phenol destruction by photocatalysis on TiO2: An attempt to solve the reaction mechanism, J. Mol. Catal. A: Chem. 213 (2004) 225–230.